Design, structural and functional characterization of a Temporin-1b analogue active against Gram negative bacteria

Concetta Avitabile,[a†] Fortuna Netti,[b†] Giuseppina Orefice,[a,c] Maddalena Palmieri,[b] Nunzia Nocerino,[c] Gaetano Malgieri,[b] Luca D. D'Andrea,[d] Rosanna Capparelli,[c] Roberto Fattorusso[b]*, Alessandra Romanelli[a]*

a:Università di Napoli "Federico II", Dipartimento delle Scienze Biologiche, via Mezzocannone 16, 80134 Napoli (Italy)

b: Seconda Università degli Studi di Napoli, Dipartimento di Scienze Ambientali, via Vivaldi 43, 81100 Caserta (Italy)

c:Università di Napoli "Federico II", Dipartimento di Scienze del Suolo, della Pianta, dell'Ambiente e delle Produzioni Animali, Via Università 133, 80055 Portici, (Italy)

d: Istituto di Biostrutture e Bioimmagini (CNR), via Mezzocannone 16, 80134 Napoli (Italy)

[†] **The authors equally contributed to the work**

***The authors share the corresponding authorship**

Corresponding authors contact details:

Alessandra Romanelli : e-mail: alessandra.romanelli@unina.it; tel +30 0812532037

Roberto Fattorusso: e-mail: roberto.fattorusso@unina2.it; tel: +39 0823274410

Abstract

Background: Temporins are small antimicrobial peptides secreted by the *Rana temporaria* showing mainly activity against Gram-positive bacteria. However, different members of the temporin family, as Temporin B, act in synergy also against Gram-negative bacteria. With the aim to develop a peptide with a wide spectrum of antimicrobial activity we designed and analyzed a series of Temporin B analogues.

Methods: Peptides were initially obtained by Ala scanning on Temporin B sequence; antimicrobial activity tests allowed to identify the TB_G6A sequence, which was further optimized by increasing the peptide positive charge (TB_KKG6A). Interactions of this active peptide with the LPS of *E.coli* were investigated by CD, fluorescence and NMR.

Results: TB_KKG6A is active against Gram-positive and Gram-negative bacteria at low concentrations. The peptide strongly interacts with the LPS of Gram negative bacteria and folds upon interaction into a kinked helix.

Conclusion: Our results show that it is possible to widen the activity spectrum of an antimicrobial peptide by subtle changes of the primary structure. TB_KKG6A, having a simple composition, broad spectrum of antimicrobial activity and a very low hemolytic activity, is a promising candidate for the design of novel antimicrobial peptides.

General significance: The activity of antimicrobial peptides is strongly related to the ability of the peptide to interact and break the bacterial membrane. Our studies on TB_KKG6A indicate that efficient interactions with LPS can be achieved when the peptide is not perfectly amphipatic, since this feature seems to help the toroidal pores formation process.

Highlights

- A new Temporin B analogue, TB_KKG6A, was designed.
- TB_KKG6A is active against Gram-positive and Gram-negative bacteria.
- The peptide strongly interacts with the LPS of *E.coli*.

- The peptide folds into a kinked helix upon interaction with LPS.

- The peptide shows very low hemolytic activity.

1. Introduction

Antimicrobial peptides (AMPs) are a primitive component of innate immune system, that are constitutively or inducibly expressed in response to invasion by pathogens [1]. AMPs are widely distributed in nature, being produced by unicellular microorganisms, plants and animals, including humans. However, the amphibian integument is one of the most documented source of antimicrobial peptides, including bombinins, negrocins, brevinins, tigerinins, esculentins and temporins [2]. In response to a variety of stimuli, these chemicals are secreted onto the skin from granular glands found under the skin surface.

AMPs have antimicrobial activity toward several different organisms such as Gram-negative and Gram-positive bacteria, viruses and fungi; moreover, some of them present antiparasitic activity and exhibit selective toxicity against cancer cells [3-5]. Because of these various pharmacological activities and of the growing multi-drug resistance of bacterial strains, AMPs have been raising considerable interest in medicinal chemistry as promising templates for the development of novel small therapeutic agents [6]. In addition, they are also recognized as a possible source of pharmaceuticals for the treatment of septic shock syndromes caused by the Gram negative bacteria lipopolysaccharide (LPS) [7, 8].

Studies performed in the presence of LPS have demonstrated that it actively regulates membrane insertion and antibacterial activities of many AMPs [9-12]. The initial attachment of AMPs to LPS might occur through ionic interactions leading to “self-promoted” peptide uptake via displacement of divalent cations [13, 14]; upon interaction, the peptides fold, intercalate the phospholipid bilayer and exert their antimicrobial activities [15].

Temporins are likely the most investigated among AMPs [16-18]. They were initially isolated from the skin of the European red frog *Rana temporaria.* They are 8–14 amino acids long, show a low

net positive charge at neutral pH (ranging from 0 to +3) and are amidated at the C-terminus, as a result of a post-translational enzymatic reaction [19].

Temporins are particularly active against Gram-positive bacteria and are not toxic to eukaryotic cells. Since their cationic nature, they target the cytoplasmic membranes of microorganisms causing cell lysis [11, 20, 21]. The lower antimicrobial activity of temporins against Gram-negative bacteria is due to the presence of the LPS on the outer membrane of these bacteria, which works as external barrier to the uptake of the peptides [22]. Temporin L (TL) and temporin-1DRa are the only members of the temporin family sharing a +3 charge that are active also against Gram-negative bacteria but possess a strong hemolytic activity [23, 24].Temporin-1a (TA) and 1b (TB) do not show activity against Gram-negative bacteria, probably because of a self-association occurring on LPS, but noteworthy, they become active when combined with a sub-inhibitory concentration of TL [16, 17, 25, 26]. Synergic effect was observed for a synthetic TB analogue in combination with TA, leading to Gram-positive and Gram-negative anti-bacterial activity [25, 26].

Temporins, as most of the AMPs, are highly membrane-active and have been hypothesized to fold upon interaction with bacterial membranes. Temporins A and L, in fact, do not have conformational preferences in aqueous buffers while they assume the conformation of a α helix in model membrane systems such as SDS and DPC [27]. The peptide amphipathic helices have one hydrophobic face, supposed to be responsible for the insertion of the peptide in the lipid bilayer, and one hydrophilic face exposing the cationic residues which interacts with the negative charges of the lipids. Studies carried out on TL and TB in the presence of micelles and of negatively charged phosphatidylglycerol (PG) as membrane models lead to the hypothesis that the peptides intercalate the phospholipid bilayer forming oligomers, similar to amyloid fibers [15]. Recently, a NMR structural study of TL and TB in the presence of the LPS has also been reported [28], confirming the hypothesis of TL antiparallel dimerization. By contrast, independent TB has populations of helical and aggregated conformations in LPS [28].

Recent studies on TA analogues highlighted that hydrophobicity and positive charge determine the antimicrobial activity of the peptide [29].

In this study we designed a series of TB analogues with the aim to improve the peptide antimicrobial activity against both Gram-negative and Gram-positive strains and then to structurally elucidate the mechanism of interaction of active peptides with LPS. The peptides were synthesized substituting one or two amino acids with an alanine and lengthening the sequence with positively charged amino acids. Among the 16 designed peptides, TB_KKG6A, shows highly increased activity against Gram negative bacteria and also a slightly increased activity against Gram positive bacteria as compared to TB, with a very low hemolytic activity. Molecular details at the basis of the interaction of TB_KKG6A with the LPS from *E. coli* were investigated via Circular Dichroism (CD), Fluorescence and NMR.

2. Materials and methods

2.1 Materials

The amino acids used for the peptide synthesis Fmoc-Ala-OH, Fmoc-Asn(Trt)-OH, Fmoc-Gly-OH, Fmoc-Ile-OH, Fmoc-Leu-OH, Fmoc-Lys(Boc)-OH, Fmoc-Pro-OH, Fmoc-Ser(OtBu)-OH, Fmoc-Val-OH, Fmoc-Ahx-OH, the Rink amide MBHA resin and the activators N-Hydroxybenzotriazole (HOBT) and O-Benzotriazole-N,N,N',N'-tetramethyl-uronium-hexafluoro-phosphate (HBTU) were purchasedfrom Novabiochem (Gibbstown, NJ, USA). Acetonitrile (ACN) was from Reidel-deHaën (Seelze, Germany) and dry N,N-dimethylformamide (DMF) from LabScan (Dublin, Ireland). All other reagents were from Sigma Aldrich (Milan, Italy). LC-MS analyses were performed on a LC-MS Thermo Finnigan with an electrospray source (MSQ) on a Phenomenex Jupiter 5μ C18 300Å,

(150x4.6 mm) column. Purification was carried out on a Phenomenex Jupiter 10μProteo 90Å (250x10mm) column. LPS of *E. coli* 0111:B4 was purchased from Sigma Aldrich.

2.2 Peptide synthesis

Peptides were synthesised on solid phase by Fmoc chemistry on the MBHA (0.54 mmol/g) resin by consecutive deprotection, coupling and capping cycles. Deprotection : 30% piperidine in DMF, 5 minutes (2x). Coupling: 2.5 equivalents of amino acid + 2.49 equivalent of HOBT/HBTU (0.45 M in DMF) + 3.5 equivalents NMM, 40 minutes. Capping: acetic anhydride/DIPEA/DMF 15/15/70 v/v/v, 5 minutes.

Peptides were cleaved off the resin and deprotected by treatment of the resin with a solution of TFA/TIS/H_2O 95/2.5/2.5 v/v/v, 90 minutes. TFA was concentrated and peptides were precipitated in cold ethylic ether. Analysis of the crudes was performed by LC-MS using a gradient of acetonitrile (0.1% TFA) in water (0.1% TFA) from 5 to 50% in 30 minutes. Purifications were performed by semipreparative RP-HPLC using a gradient of acetonitrile (0.1% TFA) in water (0.1% TFA) from 5 to 50% in 30 minutes. (See Supplementary information-Table S1 for mass spec results).

2.3 NBD conjugation

To the resin bound peptide the Fmoc-Ahx-OH linker was coupled and Fmoc deprotected following standard procedures for peptide synthesis. NBD-Cl (5 eq.) was dissolved in DMF, NMM (7 eq) was

added; the solution was reacted with the peptide 3 hours at r.t. and double couplings were performed.

Peptides were cleaved off the resin and deprotected by treatment of the resin with a solution of TFA/TIS/H_2O 95/2.5/2.5 v/v/v, 90 minutes. TFA was concentrated and peptides were precipitated in cold ethylic ether. Analysis of the crudes was performed by LC-MS using a gradient of acetonitrile (0.1% TFA) in water (0.1% TFA) from 30 to 70% in 30 minutes. Purification was performed by semipreparative RP-HPLC using a gradient of acetonitrile (0.1% TFA) in water (0.1% TFA) from 30 to 70% in 30 minutes.

2.4 Circular dichroism

Circular dichroism (CD) spectra were recorded at 25° C using a 1 cm quartz cell with the Jasco-810 spectropolarimeter using a 260 – 195 nm measurement range, 100 nm/min scanning speed, 1 nm bandwidth, 4 sec response time, 0.5 nm data pitch.

Peptides concentration for CD measurement was 5 μM. CD spectra were registered in 10 mM sodium phosphate buffer, pH 7.4 and in 10 mM sodium phosphate, 20 mM SDS buffer pH 7.4. LPS titrations were carried out recording the CD spectra of the peptide TB_KKG6A in the presence of increasing concentrations of LPS at 25°C, up to a molar ratio LPS/peptide 2:1.The peptide was dissolved in Phosphate buffer 10 mM pH 7 at a 5 μM concentration; the LPS was dissolved in Phosphate buffer 10 mM pH 7 at a 50 μM concentration, before use it was subjected to temperature cycles between 4° and 70°C, interrupted by vortexing (10 minutes). The sample was stored at 4°C overnight.

2.5 Fluorescence Studies

LPS titrations were carried out monitoring the fluorescence intensity at 530 nm of the peptide TB_KKG6A-NBD in the presence of increasing concentrations of LPS, up to a 2:1 LPS/ peptide molar ratio. The excitation wavelength was set at 487 nm. The peptide was dissolved in Phosphate buffer 10 mM pH 7 at a 0.5 μM concentration, the LPS was dissolved in Phosphate buffer 10 mM pH 7 at a 5 μM concentration. All experiments were repeated in duplicate.

2.6 ITC studies

Calorimetric studies were carried out on a Microcal ITC200 GE instrument. LPS was dissolved in degassed 50mM Phosphate buffer pH 6.8, subjected to temperature cycles between 4° and 70°C, interrupted by vortexing (10 minutes) [30]. The sample was stored at 4°C overnight. The titration sequence involved 30 injections at 4 minutes intervals of 1 μL aliquots of TB_KKG6A (2mM) dissolved in Phosphate buffer 50 mM pH 6.8 into the sample cell filled with 280 μL of LPS 50 μM in Phosphate buffer 50 mM pH 6.8 at 37°C and 350 rpm. The experiment was carried out in triplicate.

2.7 Bacteria

The study included the following species: *Staphylococcus aureus* (isolate A170), *Staphylococcus epidermidis*, *Salmonella typhimurium* (*S. typhimurium*), *Escherichia coli*. Isolates were obtained from patients hospitalized at the Medical School of the University of Naples. Specimen were confirmed by PCR assay of the genes sea (*S. aureus*), fliC (*S. typhimurium*), sat (*E. coli*), ureD *S. Epidermidis* [31-33].

2.8 Antibacterial activity

Bacteria were grown at 37°C in TSB (*S. aureus* and *S. epidermidis*) or in LB medium (the remaining bacterial species), harvested while in exponential phase (OD600 nm; 0-6-0.8), centrifuged ($8x10^3$ g for 10 min), washed with saline (0.15 M NaCl), resuspended in Muller Hinton (MH) broth at the concentration of approximately $2x10^6$ CFU/mL and distributed, in triplicate, into 96 well plates (60 μL/well), mixed with increasing concentrations of the antimicrobial peptides dissolved in sterile distilled water (5–400 μg/mL, 40 μL/well) and incubated at 37°C for 20 h. The minimal peptide concentration at which 100% inhibition of microbial growth was observed, is defined as MIC and determined by measuring the absorbance at 540 nm (Biorad microplate reader model 680, Hercules, CA).

2.9 Test of the hemolytic activity of the antimicrobials

TB_KKG6A was tested for its hemolytic activity using mouse red blood cells. The blood was collected from the tail of the animals, centrifuged ($4x10^2$ g for 3 min) and washed with saline. A 4% suspension of mouse red blood cells was mixed with the peptide (from 5 μg/mL to 45 μg/mL) and incubated for 1 h at 37°C. The hemolytic activity was measured according to the formula ($OD_{peptide} - OD_{negative\ control}$)/($OD_{positivecontrol} - OD_{negative\ control}$) x100 where the negative control (0% haemolysis) is represented by erythrocytes suspended in saline and the positive control (100% haemolysis) is represented by the erythrocytes lysed with 1% triton X100 [34].

2.10 NMR Spectroscopy

The samples for NMR spectroscopy were prepared by dissolving the appropriate amount of peptide in 0.50 mL of ^1H_2O, 0.05 mL of ^2H_2O.

The NMR experiments were acquired at 298 K on a Varian Unity INOVA 500 MHz spectrometer at Dipartimento di Scienze Ambientali of Second University of Naples.

NMR experiments were processed using Varian (VNMR 6.1B) software. ^1H chemical shifts were calibrated using TMS. The program XEASY was used to analyze and assign the spectra.

The interaction of TB_KKG6A peptide with LPS was examined by recording series of one dimensional proton NMR spectra whereby 0.5 mM of TB_KKG6A in aqueous solution, pH 4.5, was titrated with various concentrations, 0.08, 0.15, 0.2 and 0.6 mg/mL of *E. coli* LPS (Sigma-Aldrich).

The 2D tr-NOESY experiments for *E. coli* LPS-bound TB_KKG6A were recorded at the LPS concentration of 0.15 mg/mL, at 298 K, which generated a large number of tr-NOE cross peaks.

The peptide/LPS complex was found to be stable over the period of data collection at these concentrations of LPS. The 2D tr-NOESY spectra were recorded at three different mixing times (150, 200 and 300 ms) with 512 increments in t1 and 2K data points in t2. The spectral width was normally 10 ppm for both dimensions.

For saturation transfer difference (STD) experiments, TB_KKG6A (0.5 mM) was dissolved in 550 μL of H_2O/D_2O and pH was adjusted to 4.5. A stock solution (1 mM) of LPS from *E. coli* was prepared in H_2O, at pH 4.5. STD experiments were performed at 298 K in the presence of 5 μM LPS using standard STD pulse sequences [35]. One-dimensional STD experiments were carried out as described previously [36, 37]. Selective saturation of LPS resonances was achieved at -2.0 ppm (40 ppm for reference spectra) using a series of 40 Gaussian-shaped pulses (49 ms, 1 ms delay between pulses), for a total saturation time of 2s. Subtraction of the two spectra (on resonance - off resonance) by phase cycling [35] leads to the difference spectrum that contains signals arising from the saturation transfer.

Paramagnetic relaxation experiments were performed by adding aliquots of 16-doxyl-stearic acid (16-DSA) (solubilized in deuterated methanol) or Mn^{2+} (dissolved in H_2O), into the samples containing the peptide-LPS complex (0.5 mM TB_KKG6A and 0.13 mg/mL *E. coli* LPS). The samples were allowed to equilibrate for 20 min before performing 2D ^1H-^1H-TOCSY experiments. The intensities of cross-peaks of TB_KKG6A in the presence of LPS were measured before and after the addition of the paramagnetic probes so that the remaining amplitudes could be calculated.

2.10 NMR derived structure calculation

NMR structures were calculated using the CYANA program [38, 39]. The tr-NOE-based distance restraints were obtained from tr-NOESY spectrum recorded with a mixing time of 150 ms. The tr-NOE cross peaks were integrated with the XEASY program and were translated to upper bound distances using the CALIBA program incorporated into the program package CYANA. Hydrogen bond constraints were not used during structure calculations. A total of 100 structures was calculated, and the 20 conformers with the lowest CYANA target function were employed for further analysis. The structures were visualized using the program MOLMOL [40]. The quality of the structures was determined using PROCHECK-NMR [41].

3 Results

3.1 Design of TB analogues and their antimicrobial activity

Peptides belonging to the temporin family share the consensus sequence XXXXXXYXXY^{+}YXX, where X=hydrophobic amino acid, Y=hydrophilic, Y^{+}=positively charged, with leucine and isoleucine being the most abundant hydrophobic amino acids and lysine the positively charged amino acid most represented [42]. In order to evaluate the role of each amino acid side chain on the peptide activity, a complete Ala scanning of TB has been executed: a series of TB analogues was obtained by substituting one or two amino acids with alanine residues (Table S1). Their antimicrobial activities were tested against Gram-positive (*S. aureus* and *S. epidermidis)* and Gram-negative (*E. coli* and *S. typhimurium*) bacteria. Functional tests indicated that TB_P3A, TB_N7A and TB_S11A preserve an antimicrobial activity comparable to TB; the other analogues lose completely their activity while, notably, TB_G6A exhibits an increased activity against Gram positive bacteria. (Table 1 and Table S2) Furthermore, as the positively charged amino acid is reported in many cases to be essential for the interaction between antimicrobial peptides and

bacterial membranes, we investigated the role of the position of the positively charged side chain; in particular, we exchanged the amino acids in positions 1 and 10 (TB_L1K_K10L) to keep constant either the charge and the amino acid content [29]. This peptide shows antimicrobial activity against Gram positive bacteria only at high concentrations (50μg/mL).

Based on these data, mutations in position 6 were analyzed to further improve the peptide activity. The side chain steric hindrance in this position was modified by synthesizing TB_G6V and TB_G6I. Their antimicrobial activities were tested and found lower than that of TB_G6A. For this reason TB_G6A was chosen for further optimization. The double mutant, TB_G6A_S11A, was analyzed to investigate the effect of widening the hydrophobic surface of the peptide; this peptide exhibits the same antimicrobial activity of TB_G6A.

Finally, the effect of increasing the positive charge on the antimicrobial activity of TB_G6A was explored, designing the peptide TB_KKG6A, which presents 2 extra lysines at the N-terminus of TB_G6A. This peptide was designed based on previous observations suggesting that the presence of two lysines at the N-terminus of another TB analogue expanded its antimicrobial activity also to Gram negative bacteria [26].Interestingly, the analogue TB_KKG6A (+4 total charge) shows an expanded spectrum of activity as compared to TB, being active against Gram negative bacteria (5μg/mL against *E. coli* and 10 μg/mL against *S. typhimurium*) and Gram positive bacteria at low concentrations. Importantly, TB_KKG6A shows very low hemolytic activity (Figure S1).

3.2 Conformational analysis of TB analogs by CD

Peptide secondary structures were determined by CD spectroscopy. All the analogues obtained by alanine scanning show the same behavior. The conformation of the peptides in phosphate buffer at pH= 7.4 is predominantly disordered, whereas in SDS micelles at pH= 7.4 they predominantly show a helical conformation (Figure S2).

TB_KKG6A CD spectra were recorded in the presence of SDS and *E. coli* LPS (Figure 1A). In SDS, TB_KKG6A is clearly in helical conformation. In the presence of *E. coli* LPS the peptide partly assumes a helical conformation.

3.3 Binding studies of TB_KKG6A to LPS by Fluorescence and CD

The interaction of TB_KKG6A with LPS was investigated by a combination of fluorescence, CD and ITC analysis. For the fluorescence experiments we employed the TB_KKG6A derivative conjugated to 7-nitrobenzo-2-oxa-1,3-diazole(NBD) (TB_KKG6A_NBD), a fluorescent probe which changes its emission in a hydrophobic environment. Fluorescence experiments carried out titrating the *E. coli* LPS into TB_KKG6A_NBD revealed a strong variation of the fluorescence intensity (Figure 2).The K_d of the peptide-*E. coli* LPS complex was found to be 47±6 nM. This value is in agreement with those obtained by fluorescence for other active antimicrobial peptides. [43] As binding of the peptide to LPS is concomitant to folding, we also calculated the binding constant plotting the CD molar ellipticity at 222 nm as a function of the LPS concentration and we obtained a similar K_d value (Figure S3).ITC experiments were carried out by titrating the peptide into the LPS at 37°C. In this conditions the binding is an exothermic process; due to inhomogeneity of the LPS samples it is not possible to determine the binding constant of the peptide to LPS by ITC (Figure 3).

3.4 NMR analysis of TB_KKG6A in aqueous solution and in presence of LPS

Sequence specific resonance assignment of all TB_KKG6A amino acids was achieved analyzing ^{1}H-^{1}H TOCSY and ^{1}H-^{1}H NOESY spectra [44]. Chemical shifts have typical random coil values (Table S3). Accordingly, the NOESY spectra of the free peptide are predominantly characterized by

intra-residue and sequential NOEs between backbone and side chain proton resonances (Figure S4), suggesting that TB_KKG6A is largely disordered in aqueous solution.

Additions of *E. coli* LPS to TB_KKG6A solution result in concentration-dependent moderate line broadening of the proton resonances without significant changes in chemical shifts (Figure 1B), indicating the binding of TB_KKG6A to LPS as confirmed by the fluorescence experiments (Figure 2). Accordingly, two-dimensional tr-NOESY spectra of TB_KKG6A obtained in the presence of sub-stoichiometric *E. coli* LPS show a significant number of NOE connectivities, suggesting a LPS-induced structural transition from a random coil state to a well-folded conformation of TB_KKG6A (Figure S5).

Residues in segments Pro3–Asn7 and Leu9–Ser11 are characterized by strong HN_i-HN_{i+1} NOEs and several medium range NOEs, such as HN_i-HN_{i+2}, $H_{\alpha i}$–HN_{i+3}, and $H_{\alpha i}$ -$H_{\beta i+3}$ correlations, typical of a helical conformation (Figure S6A,B) [44]. Noteworthy, the absence of NOE contacts involving residues which are far apart in the molecular structure indicates that the peptide in the presence of LPS very likely does not undergo self-association.

A total of 171 NOEs was obtained from the tr-NOESY spectra; these NOEs resulted in 129 meaningful distance constraints (103 inter-residues, 26 intra-residues) and 67 angle constraints which were used for the structure calculations. All the constraints (Table 2) were used to generate a total of 100 structures, among which the 20 with the lowest target function were selected and energy minimized. The obtained structures satisfied the NMR spectroscopic constraints, with no NOE violations greater than 0.2 Å. In Figure 4, the sausage representation of TB_KKG6A bound to *E. coli* LPS NMR ensemble of structures is shown. TB_KKG6A structure is well defined as the RMSD for residues Leu2-Leu12 is 0.34 Å.

The peptide TB_KKG6A in the presence of *E. coli* LPS assumes mostly a helical conformation; in detail, a first helical segment encompassing residues Pro3 to Asn7, is followed by a kink including residue Leu8 and by a second helical region from residue Leu9 to Ser11. The angle between the two

helix axes is about 100°. Interestingly, TB_KKG6A structure shows a certain degree of amphipathicity that characterizes mainly the central tract of the peptide (Figure 5).

3.5 Structural characterization of TB_KKG6A-*E. coli* LPS interaction by STD

A close proximity of TB_KKG6A with *E. coli* LPS was revealed from saturation transfer difference (STD) NMR studies [35]. In the STD spectrum of TB_KKG6A (Figure S7) all the side chain proton resonances were observed, indicating that the entire peptide is closely associated with LPS. Unambiguous STD effects were assigned to Pro3, Asn7 and Lys10 resonances. In particular, $H_{\delta 3}$ of Pro3 and H_{β} of Asn7 show a moderate STD effect (25% and 35%) while a stronger STD effect is observed for $H\gamma$ of Lys10 (63%) (Figure S8), suggesting a closer proximity of Lys10 and at a lesser extent of Pro3 and Asn7 to LPS.

3.6 Topological Orientation of TB_KKG6A by NMR Paramagnetic Relaxation Enhancement (PRE)

In order to determine the positioning of TB_KKG6Awith respect to the LPS, an internal paramagnetic mapping was carried out on the peptide-LPS solution. The 16-doxylstearic acid (16-DSA) was used as internal probe. Its unpaired electrons lead to dramatically accelerated longitudinal and transverse relaxation rates of protons in spatial proximity via highly efficient spin and electron relaxation. Therefore, this paramagnetic probe was expected to cause a broadening of the NMR signals and a decrease in resonance intensities of the residues deeply buried in the (16-DSA). [45, 46]Side chain resonances, mostly H_{β} protons of Pro3, Ala6, Asn7, Lys10, Leu12 and Leu13, are selectively reduced, indicating that these residues are closer to 16-DSA paramagnetic probe and likely penetrate the LPS through their side chains, defining a clear interaction surface

(Figures 6 and Figure S8). Furthermore, the effect of 16-DSA was observed also for the H_ε protons of Lys_{-1} and Lys10 that are differently affected by the paramagnetic probe and confirms that Lys_{-1} side chain lies on the surface of the LPS, whereas Lys10 side chain is able to penetrate it. Interestingly, TB_KKG6A structure reveals that Lys10 side chain populates two different conformational families, one directed to the solvent bulk and the other embedded into the LPS (Figure 6). The larger perturbation of Lys10 H_βs with respect to that of H_εs reflects the conformational mobility of that side chain that does not involve Lys10 H_β protons but do comprise Lys10 H_ε protons (Figure 6). These data are confirmed by the complementary paramagnetic effects observed in the presence Mn^{2+} ion (data not shown).

4 Discussion and Conclusions

Studies carried out on natural and rationally designed antimicrobial peptides highlighted the importance of the hydrophobicity and the positive charge in the determination of the structure and the antimicrobial activity of AMPs. As a matter of fact, these two factors play a key role in the peptide ability to properly interact with the outer membrane constituents of bacterial cells and to form pores within the membrane [47]. Interaction with the outer leaflet represents in most cases a crucial step to accomplish the peptide antimicrobial activity, although other mechanisms accounting for peptide antimicrobial activity have been proposed [43, 48]. Therefore, structural investigations of antimicrobial peptides in complex with LPS, a major component of the bacterial membranes, are essential to fully understand their mechanism of action [49, 50].

In this study TB analogues were designed to increase the peptide antimicrobial activity against both Gram negative and Gram positive strains and molecular details of the interaction between the active designed peptides and LPS were obtained at an atomic resolution.

To better understand the role of each side chain on the peptide activity a complete Ala scanning of TB was executed. Functional tests indicated that TB_P3A,TB_G6A, TB_N7A and TB_S11A preserve antimicrobial activities against Gram.positive bacteria, whereas the other analogues completely lose their activity (Table 1). These results indicate that mutation in alanine is not detrimental to the peptide antimicrobial activity when the substituted side chain has a comparable or smaller dimension. This is an indication that the side chain dimensions play a clear role in the peptide functionality. Interestingly, replacement of glycine in position 6, leads to the most active peptide, TB_G6A, among the studied temporin analogues. On the other hand, introduction of larger hydrophobic amino acids in position 6 (TB_G6V and TB_G6I) revealed that further increase of side chain steric hindrance does not improve the recognition of the bacterial membrane.

Lys10 plays a pivotal role for the antimicrobial activity of TB against Gram-positive bacteria, since it likely anchors the peptide to the membranes, interacting with the negatively charged phospholipids. Accordingly, the TB_K10L analogue is inactive, whereas the derivative TBK1L_L10K, in which the charge and composition are invariant with respect to TB, shows antimicrobial activity against Gram- positive bacteria only at high concentrations.

All the peptides obtained by Ala scan are not active against Gram-negative bacteria such as *S. typhimurium* and *E. coli*. To further improve its antimicrobial activity, the most active TB_G6A was further modified adding two extra lysines at the N-terminus in order to verify the effect of increasing the positive charge of the peptide. The resulting peptide, TB_KKG6A (with a +4 charge), has antimicrobial activity against Gram positive bacteria comparable to that of the other analogues, but interestingly, it also exhibits significant activity against Gram negative bacteria at low concentrations, without showing hemolytic activity. TB_KKG6A was therefore chosen for a detailed structural investigation. CD analyses revealed that the peptide contains a significant degree

of helical conformation in the presence of *E. coli* LPS (Figure 1).High resolution structure of TB_KKG6A in the presence of *E. coli* LPS was determined by NMR. TB_KKG6A bound to LPS has a non-compact helical structure defined by two short helices, one spanning residues Pro3–Asn7 and a much shorter one at the C-terminus that spans residues Leu9–Ser11 (Figure 4). TB_KKG6Astructure shows only partial amphipathicity, mostly confined to the central region of the peptide chain (Figure 5), which likely contributes to its non-hemolytic activity. Fluorescence, CD and ^{1}H-NMR experiments, carried out by titrating *E. coli* LPS into TB_KKG6A, provided details at molecular level of the interaction between TB_KKG6A and the LPS, revealing a high affinity interaction of the peptide for this LPS. The binding of antimicrobial peptides to LPS is a very complicate process, which causes a reorganization of the LPS/lipid A structure from the original unilamellar/cubic into a multilamellar one; in some cases a transition of gel to liquid crystalline phase of the LPS, which also depends on the temperature, has been observed upon interaction of the endotoxin with antimicrobial peptides [51, 52]. In this study, through different techniques, in particular fluorescence by which we monitor the changes in the peptide environment due also to variation in the LPS structure, and CD by which we observe changes into the peptide secondary structure upon interaction with LPS, we obtained comparable values for the binding constant of the peptide to LPS (respectively 47±6 and 27±13 nM). These values are consistent with those of other active antimicrobial peptides obtained using fluorescence spectroscopy [25]. ITC experiments, carried out at 37°C, revealed that binding of the peptide to LPS is an exothermic process, driven by the electrostatic interactions between the positively charged peptide and the negatively charged LPS as observed for other antimicrobial peptides reported in the literature [51, 53, 54].

Atomic resolution interaction and localization of TB_KKG6A on the surface of *E. coli* LPS were characterized by STD and PRE experiments, providing molecular insights into the mechanisms by which the peptide exerts its antimicrobial activity.

In particular, our structural data describe TB_KKG6A conformational propensities required for the carpeting of the LPS outer leaflet. The extra Lys residues (Lys_{-1} and Lys_{-2}) of TB_KKG6A lie on the external surface of the LPS, anchoring the peptide to the bacterial membranes by interacting with the negatively charged phospholipids [55] and likely contribute to prevent the peptide oligomerization. Furthermore, STD and DSA paramagnetic mapping data clearly indicate that Pro3, Ala6, Asn7, Leu12 and Leu13 side chains permeate the LPS, allowing Lys10 long and amphipathic side chain to penetrate the surface. The two conformations observed for the Lys10 side chain reasonably account for the initial absorption and the subsequent insertion of the peptide into the LPS. Interestingly, Gly to Ala substitution improves TB_KKG6A hydrophobicity at the peptide-LPS interface which includes also Pro3 and Asn7 that can be mutated to Ala without affecting TB antimicrobial activity (Table 1). Overall, TB_KKG6A-LPS interaction stabilizes two short helical structures having some degree of amphipathicity in the peptide central region. These structural features propose possible implication in TB_KKG6A pore formation capability. In particular, TB_KKG6A structure in *E. Coli* LPS is only partially helical, amphipathic and relatively short to span an unperturbed phospholipid bilayer, therefore suggesting the formation of disordered toroidal pores when the peptide is incorporated inside the bacterium membranes. Accordingly, Mihalovic and Lazaridis compared the pore formed by magainin and melittin and showed that the distribution of positive charges at the peptide N-terminus and imperfect amphipathicity appears to facilitate the formation of toroidal pores, attracting LPS head groups and pulling them into the pore[47]. Concomitantly, the presence of positively charged side chains in the middle of the peptide results in more disordered pores.

It has been proposed that helicity of the AMPs is one of the key features for their hemolytic but not for their antimicrobial activity [56]. A strong hemolytic activity generally correlates with high hydrophobicity, high amphipathicity, and high helicity. In addition, a higher ability to self-associate in solution is generally correlated with weaker antimicrobial activity and stronger hemolytic activity of the antimicrobial peptides [56].In this frame the here reported monomeric and partially helical

and amphipathic structure of TB_KKG6A appears to answer to the structural requirements necessary to increase the antimicrobial activity and reduce toxicity to eukaryotic cells.

Interestingly the composition of the LPS is crucial for the recognition and folding processes by the peptide. In fact, CD experiments carried out for TB_KKG6A in the presence of *S. typhimurium* LPS variant with shorter sugar chains at distal region of the O-antigen moieties show that in this case the peptide has a low, although clearly visible, content of secondary structure (manuscript in preparation).

In summary, the experiments described in this study have highlighted the possibility to widen the original spectrum of action of AMPs selective for Gram-positive bacteria to Gram-negative bacteria by appropriate changes in the peptide primary structure. By combining CD, NMR and fluorescence analyses we obtained a molecular-level resolution of the TB_KKG6A structure and of its interaction with *E. coli* LPS. Our finding show that TB_KKG6A, having a simple composition, broad spectrum of antimicrobial activity and no hemolytic activity, is a promising candidate for the design of novel antimicrobial peptides with improved antimicrobial activity and very low hemolytic effect.

Figures

Figure 1: A) CD spectra of TB_KKG6A (5 μM) recorded in Phosphate buffer 10 mM pH 7.0 (blue curve), *E. coli* LPS, peptide/LPS 1:1 molar ratio (green line), B) Low-field region of one-dimensional ^{1}H NMR spectra of 0.5 mM TB_KKG6A in aqueous solution (pH 4.5) (bottom) and in the presence of *E .coli* LPS (0.05 mg/mL)(top). Line-broadening effect (R_2) of TB_KKG6A in the presence of LPS indicates that the peptide binds to the LPS.

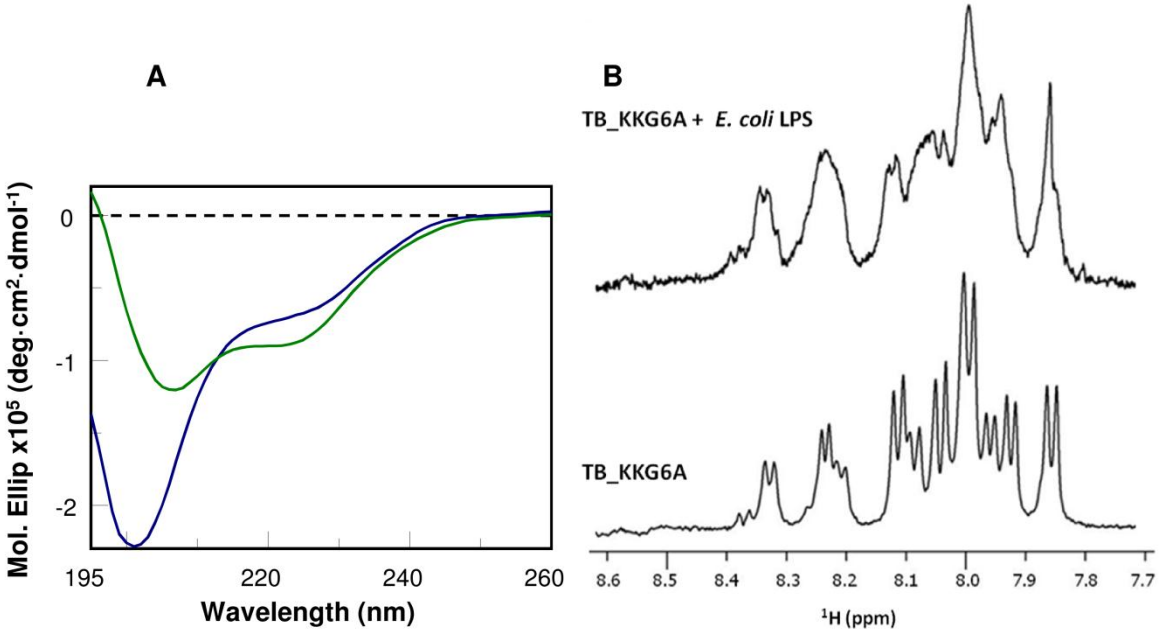

Figure 2: Titration of *E. coli* LPS into TB_KKG6A followed by fluorescence. *E .coli* LPS (5 μM) was titrated into a TB_ KKG6A _NBD (0.5 μM) up to a molar ration LPS/peptide 2:1.Deviations are not visible for some points since their magnitude is smaller than the circles reported for the experimental points.

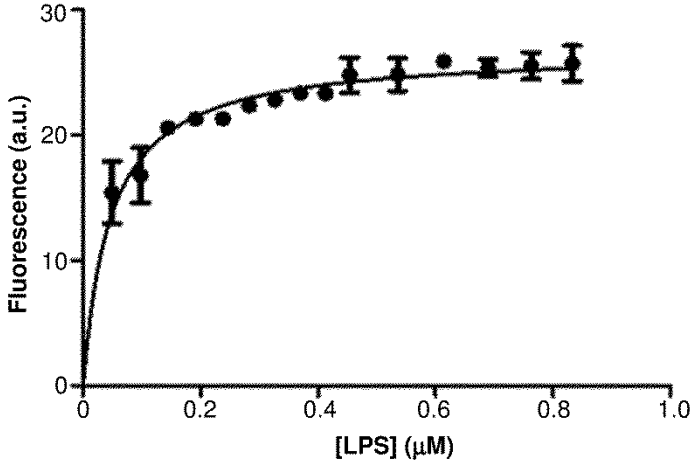

Figure 3: Titration of TB_KKG6A (2 mM) into LPS (50 μM) at 37°C followed by ITC.

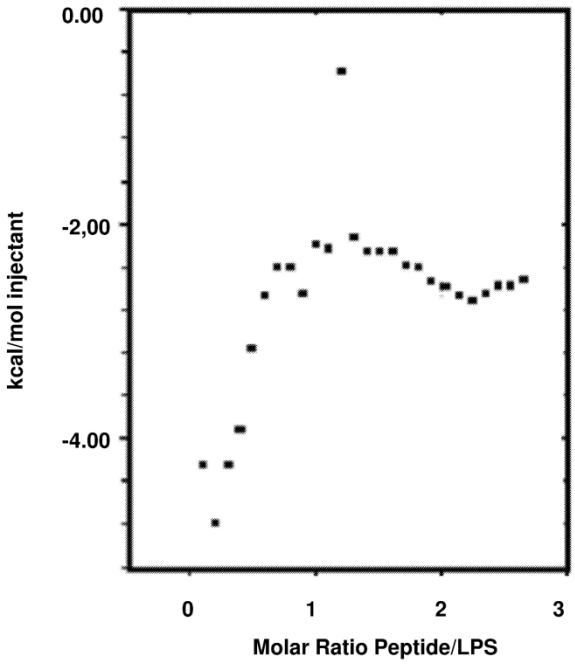

Figure 4: Left. Sausage representation of TB_KKG6A bound to *E. coli* LPS NMR ensemble of structures. **Right.** The side-chains orientation of a representative NMR structure of TB_KKG6A bound to *E. coli* LPS.

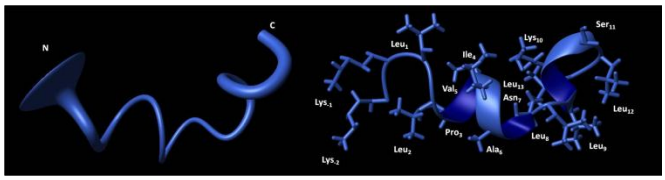

Figure 5: Surface representation showing the electrostatic surface potentials of the peptide TB_KKG6A bound to *E. coli* LPS. The hydrophobic surfaces are colored in light gray, positively charged residues in blue.

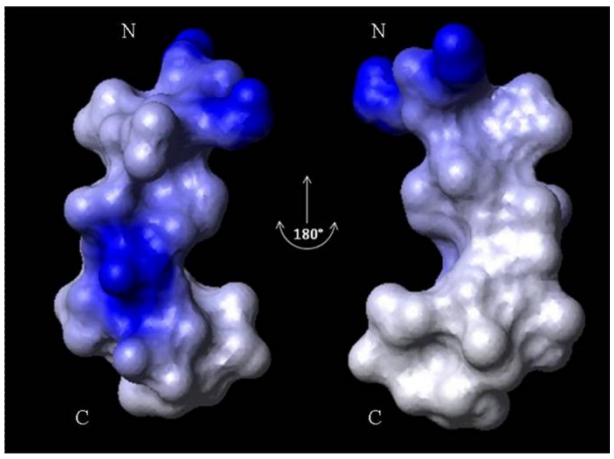

Figure 6: Mapping of paramagnetic probes induced resonance perturbation of TB_KKG6A in LPS. The yellow side-chains are located inside the LPS, as demonstrated by 16-DSA perturbation. Lys10 has a double conformation as showed in the two selected conformers.

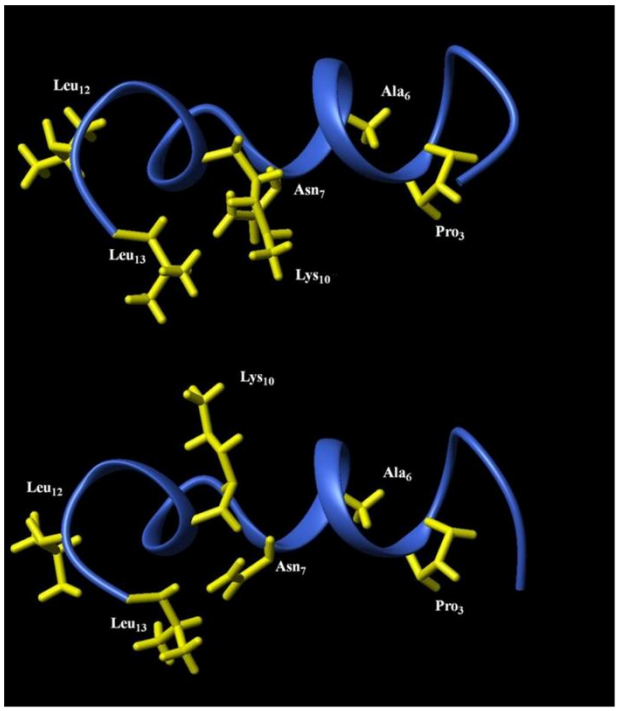

References

[1] H.G. Boman, Peptide antibiotics and their role in innate immunity, Annu Rev Immunol, 13 (1995) 61-92.
[2] A.C. Rinaldi, Antimicrobial peptides from amphibian skin: an expanding scenario, Current opinion in chemical biology, 6 (2002) 799-804.
[3] D.W. Hoskin, A. Ramamoorthy, Studies on anticancer activities of antimicrobial peptides, Biochim Biophys Acta, 1778 (2008) 357-375.
[4] N. Papo, Y. Shai, Host defense peptides as new weapons in cancer treatment, Cell Mol Life Sci, 62 (2005) 784-790.
[5] A. Mor, Multifunctional host defense peptides: antiparasitic activities, Febs J, 276 (2009) 6474-6482.
[6] H.A. Pereira, Novel therapies based on cationic antimicrobial peptides, Current pharmaceutical biotechnology, 7 (2006) 229-234.
[7] B.B. Finlay, R.E. Hancock, Can innate immunity be enhanced to treat microbial infections?, Nature reviews. Microbiology, 2 (2004) 497-504.
[8] R.E. Hancock, A. Patrzykat, Clinical development of cationic antimicrobial peptides: from natural to novel antibiotics, Current drug targets. Infectious disorders, 2 (2002) 79-83.
[9] Y. Rosenfeld, Y. Shai, Lipopolysaccharide (Endotoxin)-host defense antibacterial peptides interactions: role in bacterial resistance and prevention of sepsis, Biochim Biophys Acta, 1758 (2006) 1513-1522.
[10] S. Bhattacharjya, A. Ramamoorthy, Multifunctional host defense peptides: functional and mechanistic insights from NMR structures of potent antimicrobial peptides, The FEBS journal, 276 (2009) 6465-6473.
[11] S.E. Blondelle, K. Lohner, Combinatorial libraries: a tool to design antimicrobial and antifungal peptide analogues having lytic specificities for structure-activity relationship studies, Biopolymers, 55 (2000) 74-87.
[12] N. Papo, Z. Oren, U. Pag, H.G. Sahl, Y. Shai, The consequence of sequence alteration of an amphipathic alpha-helical antimicrobial peptide and its diastereomers, J Biol Chem, 277 (2002) 33913-33921.
[13] H. Nikaido, Prevention of drug access to bacterial targets: permeability barriers and active efflux, Science (New York, N.Y.), 264 (1994) 382-388.
[14] R.E. Hancock, Alterations in outer membrane permeability, Annual review of microbiology, 38 (1984) 237-264.
[15] A.K. Mahalka, P.K. Kinnunen, Binding of amphipathic alpha-helical antimicrobial peptides to lipid membranes: lessons from temporins B and L, Biochim Biophys Acta, 1788 (2009) 1600-1609.
[16] M.L. Mangoni, Y. Shai, Temporins and their synergism against Gram-negative bacteria and in lipopolysaccharide detoxification, Biochim Biophys Acta, 1788 (2009) 1610-1619.
[17] M.L. Mangoni, R.F. Epand, Y. Rosenfeld, A. Peleg, D. Barra, R.M. Epand, Y. Shai, Lipopolysaccharide, a key molecule involved in the synergism between temporins in inhibiting bacterial growth and in endotoxin neutralization, J Biol Chem, 283 (2008) 22907-22917.
[18] A. Romanelli, L. Moggio, R.C. Montella, P. Campiglia, M. Iannaccone, F. Capuano, C. Pedone, R. Capparelli, Peptides from Royal Jelly: studies on the antimicrobial activity of jelleins, jelleins analogs and synergy with temporins, J Pept Sci, 17 (2011) 348-352.
[19] A.F. Bradbury, D.G. Smyth, Peptide amidation, Trends in biochemical sciences, 16 (1991) 112-115.
[20] Y. Shai, Mode of action of membrane active antimicrobial peptides, Biopolymers, 66 (2002) 236-248.
[21] A. Bhunia, A. Ramamoorthy, S. Bhattacharjya, Helical hairpin structure of a potent antimicrobial peptide MSI-594 in lipopolysaccharide micelles by NMR spectroscopy, Chemistry, 15 (2009) 2036-2040.
[22] M. Zasloff, Antimicrobial peptides of multicellular organisms, Nature, 415 (2002) 389-395.
[23] A.C. Rinaldi, M.L. Mangoni, A. Rufo, C. Luzi, D. Barra, H. Zhao, P.K. Kinnunen, A. Bozzi, A. Di Giulio, M. Simmaco, Temporin L: antimicrobial, haemolytic and cytotoxic activities, and effects on membrane permeabilization in lipid vesicles, Biochem J, 368 (2002) 91-100.
[24] J.M. Conlon, N. Al-Ghafari, L. Coquet, J. Leprince, T. Jouenne, H. Vaudry, C. Davidson, Evidence from peptidomic analysis of skin secretions that the red-legged frogs, Rana aurora draytonii and Rana aurora aurora, are distinct species, Peptides, 27 (2006) 1305-1312.

[25] Y. Rosenfeld, D. Barra, M. Simmaco, Y. Shai, M.L. Mangoni, A synergism between temporins toward Gram-negative bacteria overcomes resistance imposed by the lipopolysaccharide protective layer, J Biol Chem, 281 (2006) 28565-28574.
[26] R. Capparelli, A. Romanelli, M. Iannaccone, N. Nocerino, R. Ripa, S. Pensato, C. Pedone, D. Iannelli, Synergistic antibacterial and anti-inflammatory activity of temporin A and modified temporin B in vivo, PLoS One, 4 (2009) e7191.
[27] A. Carotenuto, S. Malfi, M.R. Saviello, P. Campiglia, I. Gomez-Monterrey, M.L. Mangoni, L.M. Gaddi, E. Novellino, P. Grieco, A different molecular mechanism underlying antimicrobial and hemolytic actions of temporins A and L, Journal of medicinal chemistry, 51 (2008) 2354-2362.
[28] A. Bhunia, R. Saravanan, H. Mohanram, M.L. Mangoni, S. Bhattacharjya, NMR structures and interactions of temporin-1Tl and temporin-1Tb with lipopolysaccharide micelles: mechanistic insights into outer membrane permeabilization and synergistic activity, J Biol Chem, 286 (2011) 24394-24406.
[29] P. Grieco, V. Luca, L. Auriemma, A. Carotenuto, M.R. Saviello, P. Campiglia, D. Barra, E. Novellino, M.L. Mangoni, Alanine scanning analysis and structure-function relationships of the frog-skin antimicrobial peptide temporin-1Ta, J Pept Sci, 17 (2011) 358-365.
[30] X. Chen, J. Howe, J. Andra, M. Rossle, W. Richter, A.P. da Silva, A.M. Krensky, C. Clayberger, K. Brandenburg, Biophysical analysis of the interaction of granulysin-derived peptides with enterobacterial endotoxins, Biochim Biophys Acta, 1768 (2007) 2421-2431.
[31] M. Ananias, T. Yano, Serogroups and virulence genotypes of Escherichia coli isolated from patients with sepsis, Braz J Med Biol Res, 41 (2008) 877-883.
[32] Y. Hong, T. Liu, M.D. Lee, C.L. Hofacre, M. Maier, D.G. White, S. Ayers, L. Wang, R. Berghaus, J.J. Maurer, Rapid screening of Salmonella enterica serovars Enteritidis, Hadar, Heidelberg and Typhimurium using a serologically-correlative allelotyping PCR targeting the O and H antigen alleles, BMC Microbiol, 8 (2008) 178.
[33] A. Pechorsky, Y. Nitzan, T. Lazarovitch, Identification of pathogenic bacteria in blood cultures: comparison between conventional and PCR methods, J Microbiol Methods, 78 (2009) 325-330.
[34] J. Lee, Y. Choi, E.R. Woo, D.G. Lee, Isocryptomerin, a novel membrane-active antifungal compound from Selaginella tamariscina, Biochem Biophys Res Commun, 379 (2009) 676-680.
[35] M. Mayer, B. Meyer, Characterization of Ligand Binding by Saturation Transfer Difference NMR Spectroscopy, Angewandte Chemie International Edition, 38 (1999) 1784-1788.
[36] A. Bhunia, H. Mohanram, S. Bhattacharjya, Lipopolysaccharide bound structures of the active fragments of fowlicidin-1, a cathelicidin family of antimicrobial and antiendotoxic peptide from chicken, determined by transferred nuclear Overhauser effect spectroscopy, Biopolymers, 92 (2009) 9-22.
[37] A. Bhunia, P.N. Domadia, S. Bhattacharjya, Structural and thermodynamic analyses of the interaction between melittin and lipopolysaccharide, Biochim Biophys Acta, 1768 (2007) 3282-3291.
[38] T. Herrmann, P. Guntert, K. Wuthrich, Protein NMR structure determination with automated NOE assignment using the new software CANDID and the torsion angle dynamics algorithm DYANA, Journal of molecular biology, 319 (2002) 209-227.
[39] P. Guntert, Automated NMR structure calculation with CYANA, Methods in molecular biology (Clifton, N.J.), 278 (2004) 353-378.
[40] R. Koradi, M. Billeter, K. Wuthrich, MOLMOL: a program for display and analysis of macromolecular structures, Journal of molecular graphics, 14 (1996) 51-55, 29-32.
[41] R.A. Laskowski, J.A. Rullmannn, M.W. MacArthur, R. Kaptein, J.M. Thornton, AQUA and PROCHECK-NMR: programs for checking the quality of protein structures solved by NMR, Journal of biomolecular NMR, 8 (1996) 477-486.
[42] D. Wade, A. Silveira, J. Silberring, P. Kuusela, H. Lankinen, Temporin antibiotic peptides: A review and derivation of a consensus sequence, Protein Peptide Lett, 7 (2000) 349-357.
[43] Y. Rosenfeld, N. Papo, Y. Shai, Endotoxin (lipopolysaccharide) neutralization by innate immunity host-defense peptides. Peptide properties and plausible modes of action, J Biol Chem, 281 (2006) 1636-1643.
[44] K. Wuthrich, NMR of proteins and nucleic acids, in, John Wiley & Sons Inc., New York, 1986, pp. 292.
[45] Z. Wang, J.D. Jones, J. Rizo, L.M. Gierasch, Membrane-bound conformation of a signal peptide: a transferred nuclear Overhauser effect analysis, Biochemistry, 32 (1993) 13991-13999.

[46] S. Galdiero, L. Russo, A. Falanga, M. Cantisani, M. Vitiello, R. Fattorusso, G. Malgieri, M. Galdiero, C. Isernia, Structure and orientation of the gH625-644 membrane interacting region of herpes simplex virus type 1 in a membrane mimetic system, Biochemistry, 51 (2012) 3121-3128.
[47] M. Mihajlovic, T. Lazaridis, Charge distribution and imperfect amphipathicity affect pore formation by antimicrobial peptides, Biochim Biophys Acta, 1818 (2012) 1274-1283.
[48] I. Nagaoka, S. Hirota, F. Niyonsaba, M. Hirata, Y. Adachi, H. Tamura, D. Heumann, Cathelicidin family of antibacterial peptides CAP18 and CAP11 inhibit the expression of TNF-alpha by blocking the binding of LPS to CD14(+) cells, J Immunol, 167 (2001) 3329-3338.
[49] L. Ding, L. Yang, T.M. Weiss, A.J. Waring, R.I. Lehrer, H.W. Huang, Interaction of antimicrobial peptides with lipopolysaccharides, Biochemistry, 42 (2003) 12251-12259.
[50] R.M. Epand, H.J. Vogel, Diversity of antimicrobial peptides and their mechanisms of action, Biochim Biophys Acta, 1462 (1999) 11-28.
[51] J. Andra, M. Lamata, G. Martinez de Tejada, R. Bartels, M.H. Koch, K. Brandenburg, Cyclic antimicrobial peptides based on Limulus anti-lipopolysaccharide factor for neutralization of lipopolysaccharide, Biochem Pharmacol, 68 (2004) 1297-1307.
[52] T. Schuerholz, K. Brandenburg, G. Marx, Antimicrobial peptides and their potential application in inflammation and sepsis, Crit Care, 16 (2012) 207.
[53] J. Andra, P. Garidel, A. Majerle, R. Jerala, R. Ridge, E. Paus, T. Novitsky, M.H. Koch, K. Brandenburg, Biophysical characterization of the interaction of Limulus polyphemus endotoxin neutralizing protein with lipopolysaccharide, Eur J Biochem, 271 (2004) 2037-2046.
[54] J. Andra, J. Howe, P. Garidel, M. Rossle, W. Richter, J. Leiva-Leon, I. Moriyon, R. Bartels, T. Gutsmann, K. Brandenburg, Mechanism of interaction of optimized Limulus-derived cyclic peptides with endotoxins: thermodynamic, biophysical and microbiological analysis, Biochem J, 406 (2007) 297-307.
[55] M. Dathe, T. Wieprecht, Structural features of helical antimicrobial peptides: their potential to modulate activity on model membranes and biological cells, Biochim Biophys Acta, 1462 (1999) 71-87.
[56] Y. Chen, C.T. Mant, S.W. Farmer, R.E. Hancock, M.L. Vasil, R.S. Hodges, Rational design of alpha-helical antimicrobial peptides with enhanced activities and specificity/therapeutic index, J Biol Chem, 280 (2005) 12316-12329.